



AN APPLICATION OF RUNGE-KUTTA DISCONTINUOUS GALERKIN METHOD FOR FLOWS WITH STRONG DISCONTINUITIES

Emre ALPMAN

Marmara University, Mechanical Engineering Department,
Göztepe Campus, Kadıköy, Istanbul, Turkey, 34722, emre.alpman@marmara.edu.tr

(Geliş Tarihi: 28. 09. 2011, Kabul Tarihi: 26. 01. 2012)

Abstract: An implementation of Runge-Kutta Discontinuous Galerkin method was performed to simulate flows with strong discontinuities. The method was tested for a planar shock tube problem with extremely strong discontinuities, and numerical solutions were compared with predictions of a finite volume method and exact solutions. It was observed that when there are strong discontinuities in the flowfield, the limiter function adopted for solution clearly affects the overall quality of the predictions. An alternative limiting strategy, which uses combination of different limiters for different flow variables, was tested and great improvements in the solutions were observed. The method was also extended to moving adaptive grids by using Arbitrary Lagrangian-Eulerian formulation. Blast waves generated by an explosion were also simulated with and without including high temperature effects for surrounding air. Despite the high temperatures encountered, using calorically perfect gas assumption for air did not produce negative consequences.

Keywords: Runge-Kutta Discontinuous Galerkin method, Blast waves, Shock tube, Strong discontinuities, Arbitrary Lagrangian-Eulerian formulation, Moving grid.

GÜÇLÜ SÜREKSİZLİKLER İÇEREN AKIŞLAR İÇİN RUNGE-KUTTA DISCONTINUOUS GALERKIN METODU UYGULAMASI

Özet: Güçlü süreksizlikleri içeren akışları simle etmek için Runge-Kutta Discontinuous Galerkin metodunun bir uygulaması yapılmıştır. Metot aşırı derecede güçlü süreksizlikler içeren düzlemsel şok tüpü probleminde denenmiş ve sayısal sonuçlar sonlu hacim yöntemiyle elde edilen tahminlerle ve kesin sonuçlarla karşılaştırılmıştır. Akış alanı içinde güçlü süreksizlikler olduğunda, kullanılan sınırlayıcı fonksiyonun sonuçların genel kalitesini belirgin bir şekilde etkilediği gözlenmiştir. Farklı akış değişkenleri için farklı sınırlayıcı kombinasyonları kullanan alternatif bir sınırlayıcı stratejisi test edilmiş ve sonuçlarla büyük iyileşmeler gözlenmiştir. Metot, Arbitrary Lagrangian-Eulerian formülasyonu kullanılarak intibak eden çözüm ağlarına da uyarlanmıştır. Patlama sonrası oluşan şok dalgaları da, etrafı saran hava için yüksek sıcaklık etkilerini ekleyerek ve ihmal ederek simle edilmiştir. Çok yüksek sıcaklıklara rastlanmasına rağmen, hava için kalorik olarak ideal gaz varsayımı yapılmasının negatif etkiler yaratmamıştır.

Anahtar Kelimeler: Runge-Kutta Discontinuous Galerkin metodu, Patlama sonrası oluşan şok dalgaları, Şok tüpü, Güçlü süreksizlikler, Arbitrary Lagrangian-Eulerian formülasyonu, İntibak eden ağ.

INTRODUCTION

High pressure and temperature gases generated by an explosion expand into the surrounding medium to generate a spherical shock wave called a blast wave (Dewey, 2001). Mainly being a moving shock wave problem, blast wave simulations can successfully be performed by defining the flowfield using Euler equations. In Refs (Alpman, 2009a, 2009b, Chen et al., 2008, Chen et al., 2007, Alpman et al., 2007) blast wave simulations were performed by solving Euler equations using a finite volume method. Discontinuous Galerkin (DG) methods, which have the features of both finite volume and finite element methods, have started to become popular for the solution of hyperbolic conservation laws like Euler equations (Cockburn,

2001). DG method represents solution on elements by a collection of piecewise discontinuous functions hence sometimes considered as a high order accurate extension of finite volume method (Cockburn, 2001). One class of DG methods is the Runge-Kutta DG method (RKDG) where spatial discretization is performed using polynomials which are discontinuous across element faces. Then the resulting system of ordinary differential equations is solved using a total variation diminishing (TVD) Runge-Kutta scheme (Gottlieb and Shu, 1998).

The details of the RKDG scheme can be found in references (Cockburn and Shu, 1989, 1991, 1998, 2001, Cockburn et al., 1989, 1990). An alternative to the RKDG method is the Space-Time Discontinuous

Galerkin Method (STDG) in which the space and time discretizations are not separated (van der Veegt and van der Ven, 2002a, 2002b). This method is particularly suitable for numerical solutions on adaptive meshes.

This study includes an implementation of RKDG method to simulate one-dimensional, moving rectangular and spherical discontinuities on static and moving grids. Predictions were compared to the results obtained using a second order accurate finite volume method.

THEORY

Euler equations in arbitrary Lagrangian-Eulerian (ALE) form can be written as (Smith, 1999)

$$\iiint_{\Omega} \frac{\partial \mathbf{q}}{\partial t} d\Omega + \iint_S \mathbf{q} (\mathbf{V}_s \cdot \mathbf{n}) dS + \iint_S \mathbf{F}_n dS = \mathbf{0} \quad (1)$$

where

$$\mathbf{q} = [\rho \quad \rho \mathbf{V} \quad \rho E]^T \quad (2)$$

$$\mathbf{F}_n = (\mathbf{V} - \mathbf{V}_s) \cdot \mathbf{n} [\rho \quad \rho \mathbf{V} \quad \rho H]^T + [0 \quad p n \quad p (\mathbf{V}_s \cdot \mathbf{n})]^T \quad (3)$$

In equations (2) and (3) ρ is the fluid density, \mathbf{V} is the fluid velocity, p is the static pressure, \mathbf{V}_s is the velocity of the control volume (Ω), \mathbf{n} is the unit normal vector to the control surface (S), E and H are the total energy and total enthalpy per unit mass as given below.

$$E = \frac{p}{\rho(\gamma-1)} + \frac{\mathbf{V} \cdot \mathbf{V}}{2} \quad (4)$$

$$H = E + \frac{p}{\rho} \quad (5)$$

In equation (4) γ is the ratio of specific heat capacities. Using Gauss Divergence Theorem (Kreyszig, 2006) equation (1) can be rewritten in differential form for one space dimension as:

$$\frac{\partial \mathbf{q}}{\partial t} + \frac{\partial \mathbf{q} u_s}{\partial r} + \frac{\partial \mathbf{f}}{\partial r} + \mathbf{h} = \mathbf{0} \quad (6)$$

with

$$\mathbf{q} = [\rho \quad \rho u \quad \rho E]^T \quad (7)$$

$$\mathbf{f} = (u - u_s) [\rho \quad \rho u \quad \rho H]^T + [0 \quad p \quad p u_s]^T \quad (8)$$

$$\mathbf{h} = \frac{s}{r} [\rho u \quad \rho u^2 \quad \rho u H]^T \quad (9)$$

Here, u_s is the velocity of the grid points. In equation (9) $s = 0$ for Cartesian coordinates, $s = 1$ for cylindrical coordinates and $s = 2$ for spherical coordinates.

The DG method is derived by multiplying equation (6) by a test function $\phi_j(r)$ and integrating over a control volume (element) (K)

$$\int_K \frac{\partial \mathbf{q}}{\partial t} \phi(r) dK + \int_K \frac{\partial \mathbf{q} u_s}{\partial r} \phi(r) dK + \int_K \frac{\partial \mathbf{f}}{\partial r} \phi(r) dK + \int_K \mathbf{h} \phi(r) dK = 0 \quad (10)$$

Using Gauss divergence theorem, the second and third integrals in equation (10) can be rewritten as:

$$\int_K \frac{\partial \mathbf{q} u_s}{\partial r} \phi(r) dK = \oint_{\partial K} \mathbf{q} u_s \phi(r) d\partial K - \int_K \mathbf{q} u_s \frac{d\phi(r)}{dr} dK \quad (11)$$

$$\int_K \frac{\partial \mathbf{f}}{\partial r} \phi(r) dK = \oint_{\partial K} \mathbf{f} \phi(r) d\partial K - \int_K \mathbf{f} \frac{d\phi(r)}{dr} dK \quad (12)$$

Here ∂K is the closed surface surrounding element K . Specifically for one space dimension equation (10) takes the following form for an element i :

$$\int_{r_{i-1/2}}^{r_{i+1/2}} \frac{\partial \mathbf{q}}{\partial t} \phi(r) dr + [\mathbf{q} u_s \phi]_{i+1/2} - [\mathbf{q} u_s \phi]_{i-1/2} - \int_{r_{i-1/2}}^{r_{i+1/2}} \mathbf{q} u_s \frac{d\phi(r)}{dr} dr + [\mathbf{f} \phi]_{i+1/2} - [\mathbf{f} \phi]_{i-1/2} - \int_{r_{i-1/2}}^{r_{i+1/2}} \mathbf{f} \frac{d\phi(r)}{dr} dr + \int_{r_{i-1/2}}^{r_{i+1/2}} \mathbf{h} \phi(r) dr = 0 \quad (13)$$

In the DG method, the numerical solution \mathbf{q} is represented using a collection of polynomials on an element. Since the polynomial continuity across element faces is not enforced, the solution may be discontinuous at the element faces and hence the flux vector \mathbf{f} may be multi-valued in the fifth and sixth terms of equation (13). This problem is overcome by replacing this flux term with numerical flux $\hat{\mathbf{f}}$, which must be a conservative and upwind flux (Cockburn and Shu, 1998, 2001). Note that equation (13) reduces to finite volume formulation for $\phi(r) = 1$ (Cockburn and Shu 1998).

Normally in a DG method the solution and the test function belongs to the space of polynomials of degree smaller or equal to some k . This way a $(k+1)$ th order accurate approximation to the solution can be obtained (Cockburn and Shu, 1998, 2001). The approximate solution can then be written as:

$$\mathbf{q}(r, t) = \sum_{j=1}^k \mathbf{q}^j(t) \phi_j(r) \quad (14)$$

where $\mathbf{q}^j(t)$ are called the degrees of freedom of \mathbf{q} and $\phi_j(r)$ are the bases of the polynomial solution space. Typically Legendre polynomials are chosen as bases because of their orthogonality property (Cockburn, 2001, van der Veegt and van der Ven, 2002a, Calle et al., 2005, Qiu and Shu, 2005). Therefore, Legendre

polynomials were also used in this study as bases below:

$$\phi_j(r) = P_j \left(\frac{2(r-r_i)}{\Delta r_i} \right) \quad (15)$$

where $\Delta r_i = r_{i+1/2} - r_{i-1/2}$ and $P_j(r)$ is the Legendre polynomial of degree j .

$$\frac{d\mathbf{q}^j}{dt} = -\frac{2j+1}{\Delta r_i} \left[\begin{aligned} &+ [\mathbf{q}u_s \phi_j]_{i+1/2} - [\mathbf{q}u_s \phi_j]_{i-1/2} - \int_{r_{i-1/2}}^{r_{i+1/2}} \mathbf{q}u_s \frac{d\phi_j(r)}{dr} dr \dots \\ &\dots + [\mathbf{f} \phi_j]_{i+1/2} - [\mathbf{f} \phi_j]_{i-1/2} - \int_{r_{i-1/2}}^{r_{i+1/2}} \mathbf{f} \frac{d\phi_j(r)}{dr} dr + \int_{r_{i-1/2}}^{r_{i+1/2}} \mathbf{h} \phi_j(r) dr = 0 \end{aligned} \right] \quad (16)$$

The above system of ordinary differential equations can be solved using a TVD Runge-Kutta method (Gottlieb and Shu, 1998). Integrals appearing in equation (16) are solved using a quadrature method.

METHODOLOGY

Numerical solutions were performed using an in-house computer code written in C language. The code solves equation (16) in Cartesian, cylindrical, and spherical coordinates and then constructs the numerical solution using equation (14). Numerical solution of equation (16) requires a numerical upwind flux function. The selected flux function affects the quality of the solution. Performance of RKDG method with different numerical fluxes can be found in (Qiu et al., 2006). Numerous different methods were used in literature for flow problems involving shock waves. Among these methods AUSM (Advection Upstream Splitting Method) -family of methods provide algorithmic simplicity by using a scalar diffusion term (Liou, 2000). Hence, unlike many other upwind type methods, AUSM-family methods do not require the knowledge of the eigenstructure of the flow problem and this helps generate very efficient implementations. In this study the AUSM+ method (Liou, 1996) was used to calculate the numerical fluxes mainly because this method has previously been used by the author for moving shock wave simulations with satisfactory results (Alpman 2009a, 2009b, Chen et al, 2007, 2008, Alpman et al, 2007). Performance of this method was also tested against performance of van Leer (van Leer, 1982), HLLE (Einfeldt, 1988) and Roe's (Roe, 1986) upwind methods. Numerical solutions were obtained for $k=1$ and 2 which correspond to second and third order spatial accuracies, respectively. The integrals in equation (16) are obtained using a quadrature method. According to (Cockburn, 1998), for a given value of k , the applied quadrature rule must be exact for polynomials of degree $2k$ for the interior of the elements and three-point Gauss-Legendre rule (Chapra and Canale, 2006) was used in that reference for $k=2$. This method however, requires calculation of flow variables at the interior locations of an element. Therefore, three-

Submitting equation (14) into equation (13) and using basis polynomials as test functions one can obtain the following set of differential equations for the degrees of freedom thanks to the orthogonality of Legendre polynomials (Cockburn and Shu, 2001):

point Simpson's rule (Chapra and Canale, 2006), which uses the flow variables at element faces and center, was also used in this study although it is exact up to the cubic polynomials only. Numerical solutions obtained using these two integration techniques were compared with each other. DG method solutions for $k > 0$ generate spurious oscillations in the vicinity of flow discontinuities (Flaherty et al., 2002). Therefore, some kind of stabilization strategy is needed. Cockburn et.al. (Cockburn 2001, Cockburn and Shu 1991, 2001) adopted a generalized slope limiter with a TVB corrected minmod limiter (Cockburn and Shu 1989), Calle et. al. used an artificial diffusion term in their stabilized discontinuous Galerkin method (Calle et al., 2005), van der Vegt and van der Ven (van der Vegt and van der Ven, 2002a) used a stabilization operator, and Qui and Shu (Qui and Shu, 2005) used WENO type limiters to avoid spurious oscillations in their studies. Slope limiting approach, which is also used in finite volume schemes, is computationally the simplest. Therefore, a slope limiting procedure was used in this study. It is known that minmod limiter is the most dissipative limiter (Roe, 1986, Sweby, 1984) and the TVB correction mentioned in (Cockburn and Shu, 1989, 1998, 2001) is problem dependent. On the other hand, Superbee limiter (Roe, 1986) is the least dissipative and is suitable for flows with very strong shocks like a blast wave (Tai et al., 1997). In this study minmod and Superbee limiters along with the Sweby limiter (Sweby, 1984), which is between Superbee and minmod limiters, were used for numerical solutions. During the limiting procedure, the ratios the successive gradients of ($j-1$)st degree of freedom of an element to the j th degree of freedom of the same element were calculated, and minimum of these ratios were supplied as input to limiting function. Then the j th degree of freedom was multiplied by the output of the limiter. This approach is similar to the one followed in (Biswas et al., 1994). The above steps yield a system of ordinary differential equations for the degrees of freedom, which was solved using a 2nd order accurate TVD Runge-Kutta scheme (Gottlieb and Shu, 1998).

RESULTS AND DISCUSSION

In this section results obtained for Sod's shock tube problem (Sod, 1978) and blast waves generated from explosion of 1 kg of TNT were displayed.

Planar Shock-Tube Problem

In this problem a stationary high pressure fluid is separated from a stationary low pressure fluid by a barrier. At $t = 0$ the barrier is removed. This leads to a shock wave and a contact discontinuity move towards the low pressure region and an expansion fan move towards the high pressure region. In this study a shock tube problem which yielded very sharp discontinuities was solved and numerical solutions were compared with the exact solutions (Sod, 1978). The initial conditions of the problem were given as follows:

$$\rho = 1 \text{ kg/m}^3, u = 0, p = 1 \times 10^5 \text{ Pa}, r \leq 2\text{m}$$

$$\rho = 0.0001 \text{ kg/m}^3, u = 0, p = 10 \text{ Pa}, r > 2\text{m}$$

These were the same conditions studied in (Tai et al., 1997) as an extremely strong discontinuity case. This case was selected because it more closely resembles a blast wave simulation problem and it constitutes an extremely difficult case for numerical methods because of large gradients in the flowfield. The problem was solved in Cartesian coordinates, size of the solution domain was 7m and both fluids were calorically perfect air. Numerical fluxes were calculated using the AUSM+ method.

Static Grid Solutions

This section contains numerical solutions obtained using a static mesh with $N = 701$ grid points. This corresponds to a mesh spacing of 1 cm. Figure 1 shows density distribution at $t = 1.2$ ms in the vicinity of the contact surface and shock wave obtained using finite volume (FV) method and RKDG method with $k = 1$ using Superbee (sb), minmod (mm) and Sweby (sw) limiters. This way both methods would have the same spatial accuracy. Exact solution was also displayed for comparison. This figure clearly shows the difficulty the methods had experienced while resolving the strong discontinuities. Predictions obtained using minmod limiter were nearly the same for FV and RKDG methods in which results showed a much smeared contact surface and over-predicted the shock location. FV method with Superbee limiter performed relatively well although the numerical solutions are on the overall poor. In order to improve the results solutions were performed on a finer mesh which was obtained by halving the mesh spacing using $N = 1401$ grid points. Density distributions for this case were displayed in Figure 2. Greatest improvement was observed for FV method with the Superbee limiter. Other solutions were also improved slightly but not as much. Overall, the RKDG method predictions were poor compared to FV method predictions obtained using the same limiter. It is also interesting to note that RKDG solutions took nearly 1.5 times more CPU time than FV

solutions although this was not a big issue for one-dimensional flow simulations.

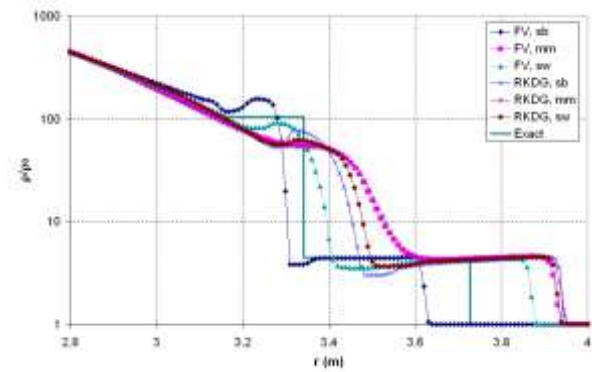


Figure 1. Density distribution at $t = 1.2$ ms. ($\rho_0 = 0.0001 \text{ kg/m}^3, N = 701$)

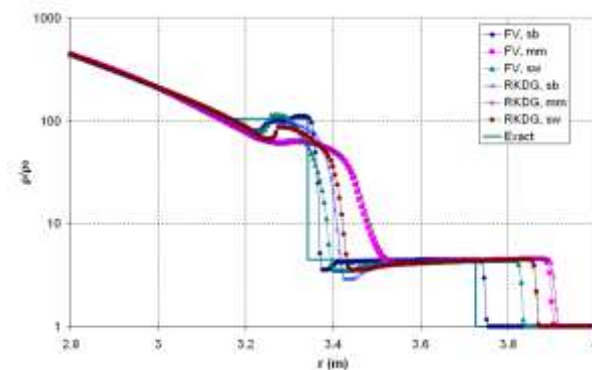


Figure 2. Density distribution $t = 1.2$ ms. ($\rho_0 = 0.0001 \text{ kg/m}^3, N = 1401$)

Pressure distributions at $t = 1.2$ ms obtained using $N = 1401$ grid points were shown in Figure 3. In this figure all numerical solutions experienced a spurious oscillation right after the expansion region. This location and the location of the shock wave are the places where discrepancies between numerical solutions were most severe. They were pretty much in agreement everywhere else in the solution domain. However, in Figure 2 there were also considerable differences between numerical solutions in the vicinity of the contact surface location which was not observed in Figure 3. Therefore, it was concluded that prediction of shock location could be improved if the contact surface could be resolved better.

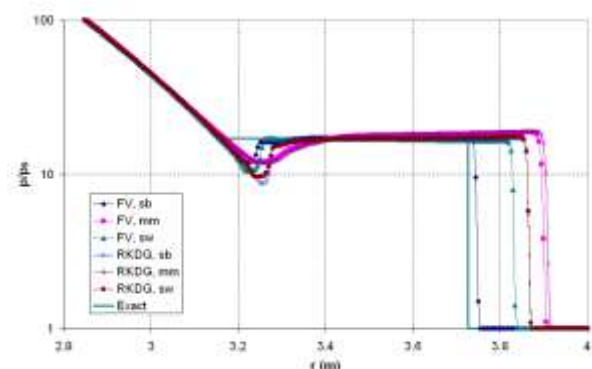


Figure 3. Pressure distribution at $t = 1.2$ ms. ($p_0 = 10 \text{ N/m}^2$)

Comparing Figure 2 and Figure 3 one can see that spurious oscillations were observed in the vicinity of the contact surface rather than the shock wave. These oscillations could be suppressed by using a more dissipative limiter however, this was shown to negatively affect the overall solution quality; solutions obtained using minmod limiter were the worst compared to others. Knowing that only density experiences a discontinuity across the contact surface while pressure and velocity remain continuous, an alternative limiting strategy was tested to see if it could improve the predictions. In this study limiting was performed on the primitive flow variables; density, velocity and pressure. Therefore, in this alternative strategy minmod limiter was applied for density only while less dissipative Superbee and Sweby limiters were applied for pressure and velocity. Density distributions obtained using this limiting strategy were displayed in Figure 4. In the figure legend first limiter was for density and second limiter was for pressure and velocity. The alternative limiting strategy, especially using minmod and Sweby limiters, improved RKDG predictions greatly. This strategy also suppressed oscillations observed in the previous FV solutions however, it negatively affected the prediction of shock location. So far, the best predictions were obtained with Superbee limiter for the FV method and with minmod-Sweby combination for the RKDG method. These predictions were compared with exact solution in Figure 5. It is clear that RKDG method with this alternative limiting successfully suppressed oscillations after the expansion region and in the vicinity of the shock wave. Also it made a slightly better shock prediction compared to FV method. Considering this improvement, RKDG solutions will employ this alternative limiting with minmod and Sweby limiters from this point forward.

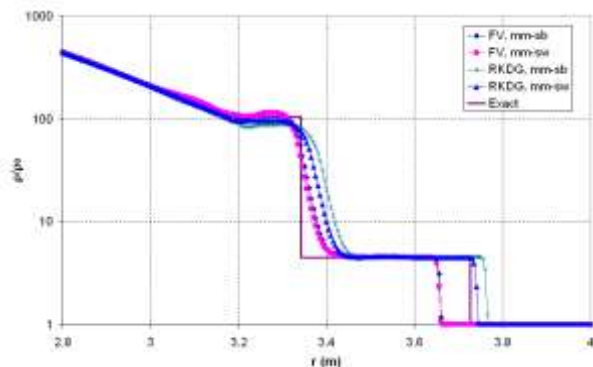


Figure 4. Density distribution at $t = 1.2$ ms. ($\rho_0 = 0.0001$ kg/m³, $N = 1401$, alternative limiting)

In order to see the effect of mesh spacing, solutions displayed in Figure 5 were repeated on the previously used coarse mesh and results were displayed in Figure 6. It is clear that RKDG solution was less sensitive to mesh spacing compared to FV method.

Spatial accuracy of RKDG methods can be easily increased by using a high order polynomial in the element. This avoids using a larger stencil as in the case

of FV or finite difference method (Cockburn and Shu, 1989). For the problem considered density distribution obtained using $k = 1$ and $k = 2$ were displayed in Figure 7. Results obtained with these two polynomials are nearly the same except $k = 2$ case placed the shock slightly ahead of the $k = 1$ case. The reason using high order polynomial did not bring much benefit is that the limiters applied degrades the high order accuracy in the vicinity of the discontinuities. This might be overcome by using a limiter which preserves the accuracy like the TVB corrected minmod limiter of Ref. (Cockburn and Shu, 1998) however that correction was problem dependent.

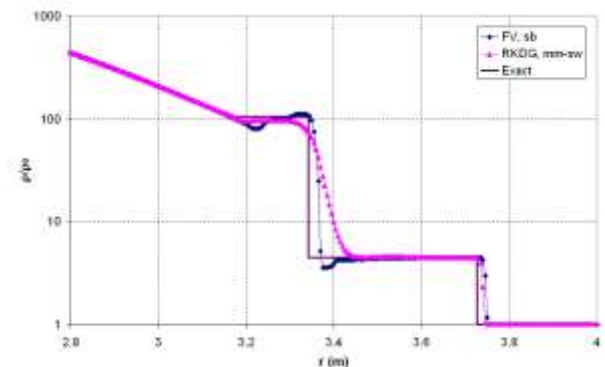


Figure 5. Density distribution at $t = 1.2$ ms. ($\rho_0 = 0.0001$ kg/m³, $N = 1401$)

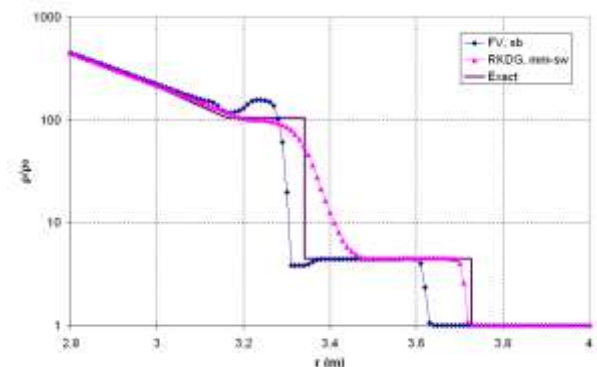


Figure 6. Density distribution at $t = 1.2$ ms. ($\rho_0 = 0.0001$ kg/m³, $N = 701$)

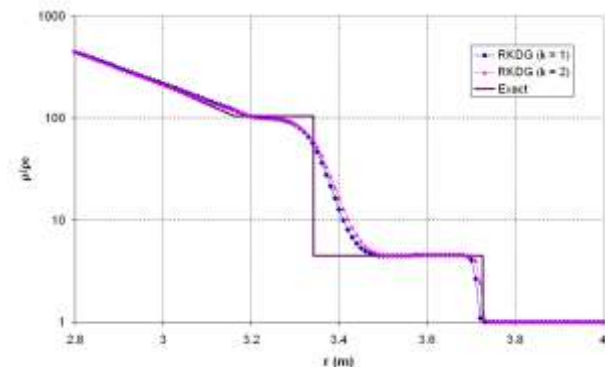


Figure 7. Density distribution at $t = 1.2$ ms obtained using $k = 1$ and 2 . ($\rho_0 = 0.0001$ kg/m³, $N = 701$)

Effect of the Quadrature Rule

Equation (16) contained integrals which were evaluated using a quadrature rule. The predictions displayed previously were obtained using three-point Simpson's rule of integration which is third-order accurate (Chapra and Canale, 2006). In order to see the effect of the quadrature rule, RKDG solution with $k = 2$ was also performed using three-point Gauss-Legendre rule (5th order accurate (Chapra and Canale, 2006)) and compared to the one with Simpson rule in Figure 8. According to the figure solution is nearly insensitive to the quadrature rule employed. Since three-point Simpson rule uses flow variables at the faces (already calculated for flux calculations) and the center of the element it does not require calculation of flow variables at the interior locations of as does three-point Gauss-Legendre rule. Therefore, it was mainly preferred and employed in this study.

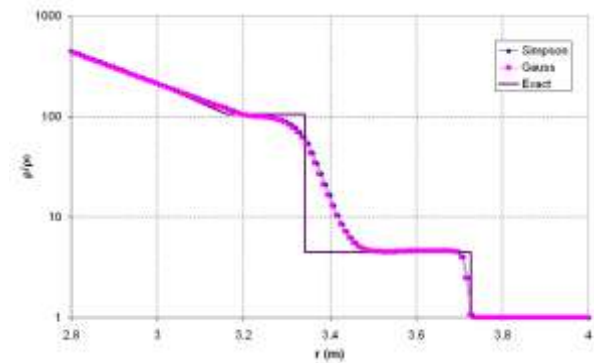


Figure 8. Density distribution at $t = 1.2$ ms obtained using different quadrature rules. ($\rho_0 = 0.0001 \text{ kg/m}^3$, $N = 701$)

Effect of Numerical Flux Function

It is also known that the numerical flux function used in the computations affects the accuracy of the DG solutions. In order to see this effect, performance of the AUSM+ method was compared to those of van Leer (VL), HLLC and Roe's methods. Density predictions obtained using these flux functions and their comparisons with the exact solution were displayed in Figure 9. According to this figure performances of these methods were close to each other except the HLLC method which clearly underpredicted the shock location. Among the flux functions tested AUSM+ showed the best performance as expected.

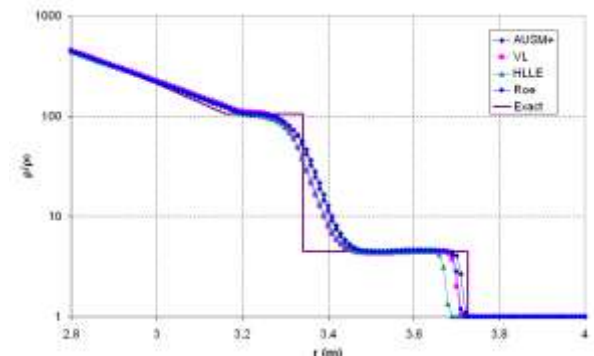


Figure 9. Density distribution at $t = 1.2$ ms obtained using different quadrature rules. ($\rho_0 = 0.0001 \text{ kg/m}^3$, $N = 701$)

Moving Adaptive Grid Solutions

Among the DG methods, STDG method (van der Vegt and van der Ven, 2002a, 2002b) provides a natural candidate for adaptive mesh solutions. This method does not separate space and time, and uses space-time elements which are obtained by connecting space elements in two consecutive time levels (van der Vegt and van der Ven, 2002a). As a result all mesh movements and deformations are automatically involved into the formulation. However, its numerical implementation may not be as straightforward as the RKDG method. Therefore, the RKDG method used in previous calculations was extended to moving meshes by using the ALE formulation described previously. Numerical solutions were obtained by solving equation (16) with the AUSM+ method for numerical fluxes. In order to adapt the grid, an arc-length type weighting function which had been previously used in (Alpman, 2009a) was also used here. This weighting function moves grid points according to the velocity gradient, hence grid points were moved so that the mesh refines in the vicinity of the shock wave. Resulting grid velocities at $t = 1.2$ and 2.8 ms were shown in Figure 10 where location of the sudden jump in velocity at a specific time is coincident with the predicted shock locations.

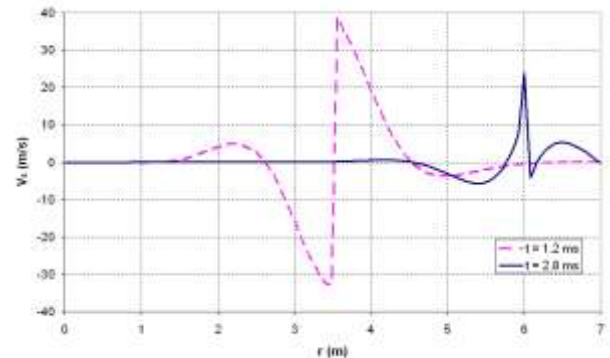


Figure 10. Grid Velocities at $t = 1.2$ and 2.8 ms.

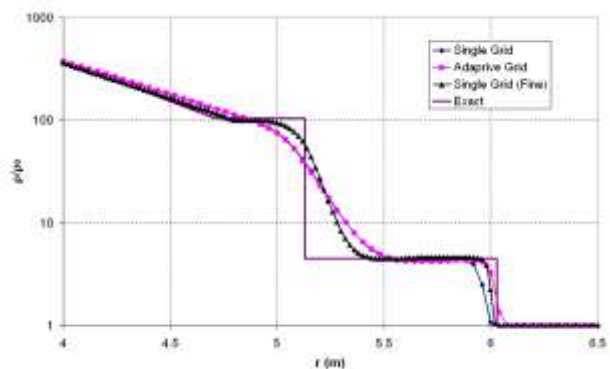


Figure 11. Density distribution at $t = 1.2$ ms obtained using static and adaptive grids. ($\rho_0 = 0.0001 \text{ kg/m}^3$, $N = 351$ for fine grid solution and 176 for other solutions)

Density distributions at $t = 2.8$ ms obtained using static grids with $N = 176$, 351 and adaptive grid with $N = 176$ were displayed in Figure 11. Since the grid is refined

around the shock wave only, numerical solutions obtained with static and adaptive grids of same size were nearly identical around the contact surface however, slightly better shock location was predicted with the latter. Overall numerical solutions were not very good, however the major aim here was not to find the best adaptive grid solution but to extend RKDG method to moving adaptive grids using ALE formulation and show that it can be successfully used as an alternative to STDG method.

Blast Wave Simulations

In this section blast waves generated by an explosion were analyzed. Here explosive material was assumed to transform gas phase instantly after the detonation, thus explosive was modeled as a high pressure sphere. This way, blast wave problem became a spherical shock tube problem where an isobaric sphere of a high pressure gas expanded toward surrounding low pressure air. Numerical solutions were obtained using RKDG method with $k = 1$, AUSM+ flux function and the alternative limiting technique which gave the best results for the planar shock tube problem analyzed in the previous section. A static grid was used with a mesh spacing of 4 mm in a 10 m solution domain.

Numerical solutions were first compared with the approximate analytic solutions of blast waves by Friedman (Friedman, 1961). The problem considered contained a sphere of air compressed to 22 times the ambient air pressure. This sphere had a non-dimensional radius of one (Sachdev, 2004). Temperature was taken to be uniform in the entire solution domain and air was assumed to be calorically perfect. Figure 12 contained loci of resulting primary shock, contact surface and secondary shock. Predictions were also compared with numerical solutions by Brode (Brode, 1957). In this figure horizontal axis represented distance from the center normalized by the initial sphere radius, r/r_0 and vertical axis represented time normalized by r_0 and ambient speed of sound, a_0 .

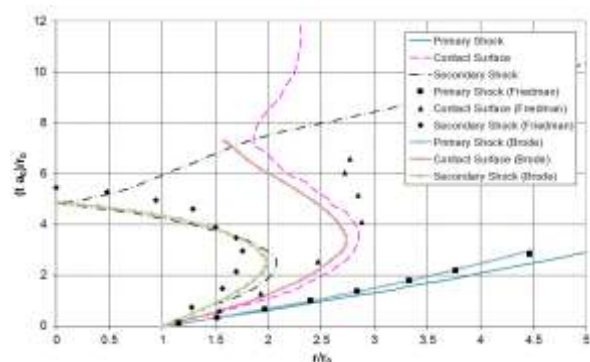


Figure 12. Loci of primary shock, contact surface and secondary shock.

According to this figure RKDG solutions showed only qualitative agreement with Friedman's approximate analytic result; however agreement with Brode's results were much better especially during the implosion of the

secondary shock and its reflection from the center. Outward motion of the secondary shock after its reflection and its interaction with the contact surface were also observed in Figure 12.

Next, blast waves generated by explosion of 1 kg of TNT were analyzed and simulated. The explosive was modeled as an isobaric high pressure sphere in which the density was 1600 kg/m^3 and pressure was 8.8447 GPa which was obtained using the blast energy of TNT (Smith and Hetherington, 1994) and the JWL (Jones-Wilkins-Lee) equation of state (Dobratz and Crawford, 1985). Outside this sphere ambient air density and pressure were 1.225 kg/m^3 and 101320 Pa, respectively. Simulations involved two different fluids; detonation products and ambient air for which different state equations were used. For detonation products JWL equation of state was used mainly due to its popularity (Kubota et al., 2007). For surrounding air two different cases were followed. First case assumed ambient air to be calorically perfect. However, after an explosion like this one ambient air temperature may easily become very high so that calorically perfect gas assumption might cease to be valid due to gas dissociations (Hoffmann and Chiang, 2000). Therefore, as the second case, high temperature effects were included by assuming local chemical equilibrium meaning that the chemical reactions occur instantaneously (Hoffmann and Chiang, 2000). Equilibrium relations given in Ref. (Tannehill and Muge, 1974) were used for air to calculate ratio of specific heat capacities and temperature in terms of pressure and density.

One of the important variables in blast wave simulation is the over-pressure, which is the rise of pressure above ambient pressure downstream of the primary shock wave. Figure 13 showed comparison of over-pressure predictions obtained for calorically perfect and equilibrium air cases with the data obtained from (Smith and Hetherington, 1994) which states that these results are curve fits to the data used in the weapons effect calculation program CONWEP (Hyde, 1991). Both cases over-predicted over-pressure with calorically perfect case being slightly better. The main discrepancy between both cases occurred between $r = 1$ and 3 m. Except this region both curves were nearly parallel.

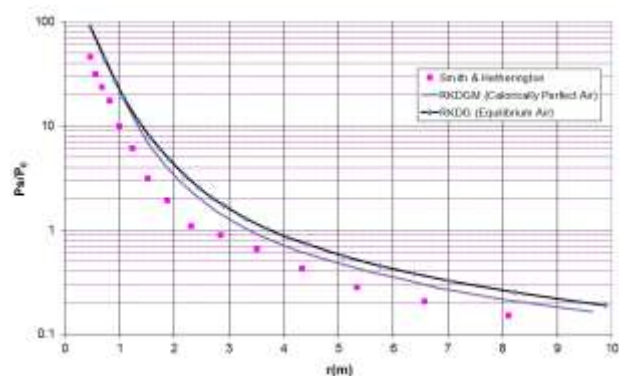


Figure 13. Variation of over-pressure with distance measured from the center.

Another important variable in blast wave simulation is the speed of the primary shock, which can be used to calculate shock arrival times. Primary shock speeds computed using RKDG method were compared with data from Ref. (Smith and Hetherington, 1994) in Figure 14. Here numerical solutions gave higher shock speeds close to the explosive but agreement with data from Ref. (Smith and Hetherington, 1994) became much better after $r = 2$ m, especially for calorically perfect air solution.

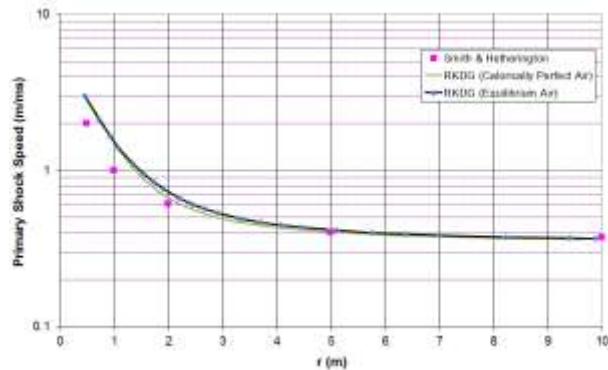


Figure 14. Variation of primary shock speed with distance from the center.

Overall solutions performed by treating air as a calorically perfect gas were in better agreement with data from Ref. (Smith and Hetherington, 1994). But it is known that high temperatures encountered during detonation of high explosives like TNT makes calorically perfect assumption invalid. Since this assumption ignores any chemical reaction that might occur, it may yield unrealistically high temperatures after a shock wave. Such problems are usually encountered for hypersonic flows over reentry vehicles (see Ref. (Anderson, 2004), chapter 16). In order to check this for our problem, temperature behind the primary shock wave predicted by the two cases of air were displayed in Figure 15. It was clear from this figure that temperatures predicted using the two assumptions were very close except in the region between $r = 1$ and 3 m, where major discrepancies between these numerical solutions took place. Since temperature predicted using calorically perfect and equilibrium air assumptions were very close, the potential negative consequences of using the former, was not experienced in this problem. Nevertheless, the predicted temperatures at lower r values were still high enough to make γ non-constant. In order to see the effect of temperature on γ , its values calculated using the equilibrium air assumption was compared with the constant value of 1.4 for calorically perfect gas assumption. This comparison was displayed in Figure 16 where a considerable drop in γ can be easily observed when r is less than 3m. This explains the relatively less pressure and temperature drop yielded by the equilibrium air assumption for the same amount of outward expansion. (See figures 13 and 15).

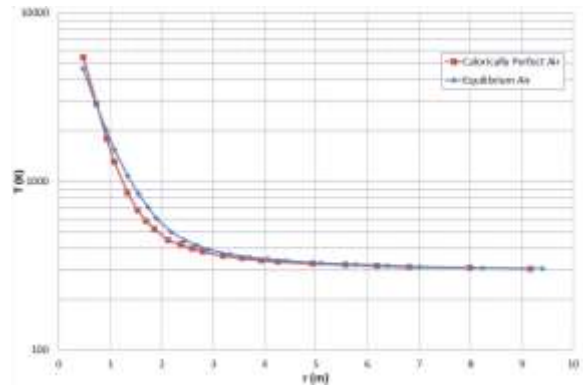


Figure 15. Variation of temperature behind primary shock with distance from the center.

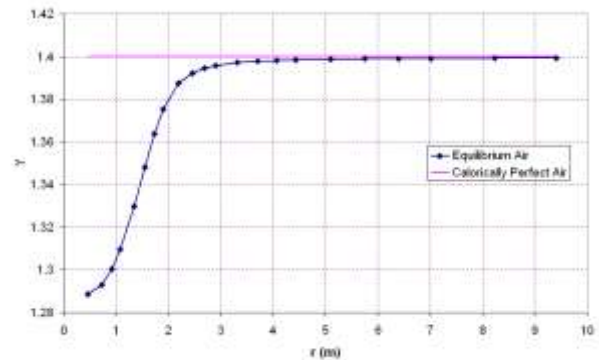


Figure 16. Variation of ratio of specific heat capacities behind primary shock with distance from the center.

RKDG predictions for blast waves represented above were obtained using the alternative limiting approach because it yielded better results for planar shock wave problem where the strength of the discontinuities remain constant. However, in a spherical shock problem the strength of the discontinuities decrease as high pressure gases expand and author's experience with planar shock tube problem with different discontinuity strengths showed that the performances of different limiting strategies became closer to each other as the discontinuity strengths decreased. In order to see the effect of limiting procedure on blast wave simulations density distributions at $t=0.1$ and 1.6 ms were plotted in Figure 17 and Figure 18 for the blast wave generated by the explosion of 1 kg of TNT. Density was plotted in order to see the contact surface. Here the ambient air was assumed to be calorically perfect air. Predictions include RKDG solutions with minmod (mm), Sweby (sw), superbee (sb) and alternative (mm for density, sw for pressure and velocity) limiters. Finite volume solution with superbee limiter was also included in the figures. According to Figure 17 RKDG solutions are very close to each other especially for secondary shock wave. The major differences are in the vicinity of the contact surface where solutions with mm and mm-sw limiters yielded more smeared contact surfaces as expected. At the same time finite volume (FV) solution showed a considerable discrepancy with RKDG solutions. Nevertheless, the strength of the discontinuity at the contact surface is small compared to that of the planar shock tube problem studied above. Therefore,

the discrepancies at the contact surface location did not affect the shock predictions considerably. This was also supported in Figure 18 which showed density distributions well after the secondary shock wave reflected from the origin and crossed the contact surface. Again RKDG predictions are very close to each other and disagreement with the FV solution is evident.

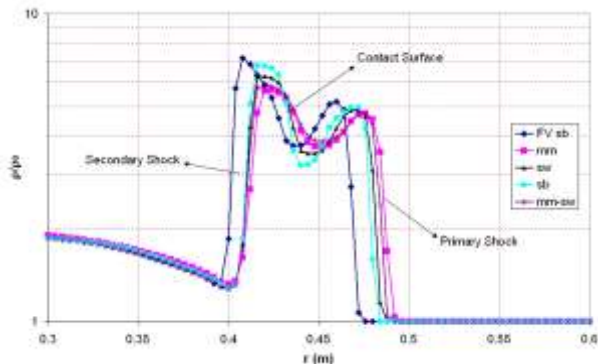


Figure 17. Density Distribution at $t=0.1$ ms.

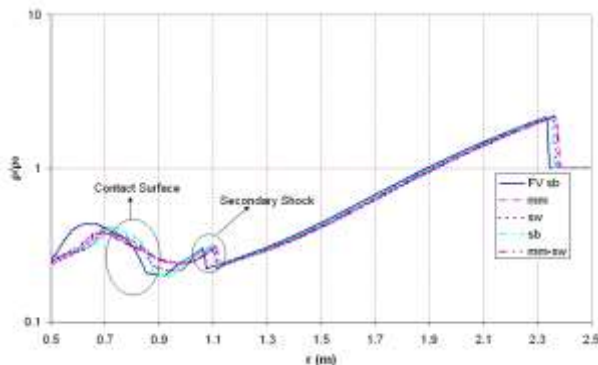


Figure 18. Density Distribution at $t=1.6$ ms.

CONCLUSIONS

An implementation of RKDG method was performed to simulate moving planar and spherical shock waves (blast waves). An in-house computational fluid dynamics code which solves Euler equations using a finite volume technique was further modified to include an RKDG method. The code was tested with a Sod's shock tube problem with the so-called extremely strong discontinuities (Tai et al., 1997). Predictions were compared with the predictions obtained using a finite volume technique and to the exact solutions. It was observed that the limiter used in the solutions clearly affected the overall quality of the predictions. The RKDG method was not able to produce satisfactory results with neither of the limiter functions used and was out-performed by FV method using the same limiter. After observing that spurious oscillations occur around the contact surface rather than the shock wave and alternative limiting strategy which used more dissipative minmod limiter (Sweby, 1984) for density and less dissipative Superbee or Sweby limiter (Sweby, 1984) for pressure and velocity was tested. This strategy clearly improved the solutions of RKDG method and RKDG with minmod-Sweby combination gave the best

results. It was interesting to see that this alternative limiting strategy did not produce a similar improvement for the FV method. Overall RKDG method with this so-called alternative limiting outperformed FV method for the analyzed shock tube problem with very strong discontinuities and it was shown to be less sensitive to grid coarsening compared to FV method.

The resulting method was tested for different flux functions and comparison of the results showed that the AUSM+ (Liou, 1996) method performed relatively better compared to the HLLC (Einfeldt, 1984), van Leer (van Leer, 1982) and Roe's (Roe, 1986) methods. The implemented method was also modified to handle moving adaptive meshes using ALE (Smith, 1999) formulation. This way the RKDG method used can be considered as an alternative to STDG (van der Vegt and van der Ven, 2002a, 2002b) method which is a natural candidate for solution on adaptive meshes.

Blast waves were simulated by modeling the explosion problem as a spherical shock tube problem. For blast wave generated by explosion of 1kg of TNT, the numerical solutions were performed with and without including the high temperature effects for the surrounding air. Although high temperatures were encountered in the solutions, using calorically perfect gas assumption for air did not produce negative effects, and even gave better agreement with blast wave data taken from Ref. (Smith and Hetherington, 1994). This may be due to the fact that equilibrium relations given in (Tannehill and Muggé, 1974) were obtained for hypersonic flow at the upper levels of the atmosphere where pressure and density is low.

REFERENCES

- Alpman E., "Blast Wave Simulations using Euler Equations and Adaptive Grids," *5th Ankara International Aerospace Conference, AIAC-2009-093*, Ankara, Turkey, August 2009a.
- Alpman E., "Simulation of Blast Waves using Euler Equations," *17th National Thermal Science and Technology Conference*, Sivas, Turkey, June 2009b. (in Turkish)
- Alpman, E., Long, L. N., Chen, C. -C., Linzell, D. G., "Prediction of Blast Loads on a Deformable Steel Plate Using Euler Equations," *18th AIAA Computational Fluid Dynamics Conference*, Miami, FL, June 2007.
- Anderson, J. D. *Modern Compressible Flow with Historical Perspective*, 3rd Edition, McGraw Hill, p. 587, 2004.
- Biswas, R., Devine, K. D., Flaherty, J. E., "Parallel, Adaptive, Finite Element Methods for Conservation Laws," *Appl. Numer. Math.*, 14, 255, 1994.

- Brode H. L., "Theoretical Solutions of Spherical Shock Tube Blasts," *Rand Corporation Report*, RM – 1974, 1957.
- Calle, J. L. D. , Devloo, P. R. B., Gomes, S. M., "Stabilized Discontinuous Galerkin Methods for Hyperbolic Equations," *Computer Methods in Applied Mechanics and Engineering*, 194, pp. 1861 – 1874, 2005.
- Chapra, S. C., Canale, R. P., *Numerical Methods for Engineers*, 5th Edition, Mc Graw-Hill, p. 626, 2006.
- Chen, C., Linzell, D. G., Long, L. N., Alpman, E., "Computational studies of polyurea coated steel plate under blast loads," *9th US National Congress on Computational Mechanics*, San Francisco, CA, July 2007.
- Chen, C.C., Alpman, E., Linzell, D.G., and Long, L.N., "Effectiveness of advanced coating systems for mitigating blast effects on steel components," *Structures Under Shock and Impact X, Book Series: WIT Transactions on the Build Environment*, 98, 85 - 94, 2008.
- Cockburn, B., "Devising Discontinuous Galerkin Methods for Non-Linear Hyperbolic Conservation Laws," *Journal of Computational and Applied Mathematics*, 128, pp. 187 – 204, 2001)
- Cockburn, B., Hou, S., Shu, C. W., "TVB Runge-Kutta Local Projection Discontinuous Galerkin Finite Element Method for Scalar Conservation Laws IV; The Multidimensional Case", *Mathematics of Computation*, 54, 545, 1990.
- Cockburn, B., Lin, S. Y., Shu, C. W., "TVB Runge-Kutta Local Projection Discontinuous Galerkin Finite Element Method for Scalar Conservation Laws III: One-dimensional Systems," *Journal of Computational Physics*, 84, 90, 1989.
- Cockburn, B., Shu, C. W., "The Runge-Kutta Discontinuous Galerkin Methods for Conservation Laws V: Multidimensional Systems," *Journal of Computational Physics*, 141, 199 – 224, 1998.
- Cockburn, B., Shu, C. W., "The Runge-Kutta Discontinuous Galerkin Methods for Convection-Dominated Problems" Review Article, *Journal of Scientific Computing*, 16, 173 – 261, 2001.
- Cockburn, B., Shu, C. W., "The Runge-Kutta Local Projection P¹-Discontinuous Galerkin Method for Scalar Conservation Laws," *M² AN*, 23, 33 , 1991.
- Cockburn, B., Shu, C. W., "TVB Runge-Kutta Local Projection Discontinuous Galerkin Finite Element Method for Scalar Conservation Laws II: General Framework," *Mathematics of Computation*, 52, 411, 1989.
- Dewey, J. M., "Expanding Spherical Shocks (Blast Waves)," *Handbook of Shock Waves*, 2, 441 – 481, (2001).
- Dobratz, B. M., Crawford, P. C., *LLNL Explosives Handbook – Properties of Chemical Explosives and Explosive Simulants*, Lawrence Livermore National Laboratory, 1985.
- Einfeldt, B., "On Godunov Type Methods for Gas-Dynamics," *SIAM Journal of Numerical Analysis*, 25, 294, 1988.
- Flaherty, J. E., Krivodonova, L., Remacle, J. F., Shephard, M. S., "Aspects of Discontinuous Galerkin Methods for Hyperbolic Conservation Laws," *Finite Elements in Analysis and Design*, 38, 889 – 908, 2002.
- Friedman, M.P., "A simplified Analysis of Spherical and Cylindrical Blast Waves," *Journal of Fluid Mechanics*, 11, 1, 1961.
- Gottlieb, S., Shu, C. W., "Total Variation Diminishing Runge-Kutta Schemes," *Mathematics of Computation*, 67, 73 – 85, 1998.
- Hoffman, K., A., Chiang, S. T., *Computational Fluid Dynamics, Volume II*, Engineering Education System™, 2000.
- Hyde, D. W., *CONWEP: Conventional Weapons Effects Program*, US Army Waterways Experimental Station, 1991.
- Kreyszig, E., *Advanced Engineering Mathematics*, John Wiley Sons, 9th edition, p. 458, 2006.
- Kubota, S., Nagayama, K., Saburi, T., Ogata, Y., "State Relations for a Two-Phase Mixture of Reacting explosives and Applications," *Combustion and Flame*, 74 – 84, 2007.
- Liou, M. -S., "A sequel to AUSM: AUSM+," *Journal of Computational Physics*, 129, 364 – 382, 1996.
- Liou, M. -S., "Mass Flux Schemes and Connection to Shock Instability," *Journal of Computational Physics*, 160, 623 – 648, 2000.
- Qiu, J., Khoo, B. C., Shu, C. W., " A Numerical Study for the Performance of the Runge-Kutta Discontinuous Galerkin Method based on Different Numerical Fluxes," *Journal of Computational Physics*, 212, 540 – 565, 2006.
- Qiu, J., Shu, C. W., "Runge-Kutta Discontinuous Galerkin Method using WENO limiters," *SIAM Journal of Scientific Computing*, 26, 907 – 929, 2005.
- Roe, P. L., "Characteristic-based Schemes for Euler Equations," *Annual Review of Fluid Mechanics*, 18, 337 – 365, 1986.

Sachdev, P. L., "Shock Waves and Explosions," *Monographs and Surveys in Pure and Applied Mathematics*, Chapman & Hall/CRC, pp. 208 – 224, 2004.

Smith, P. D., Hetherington J. D., *Blast and Ballistic Loading of Structures*, Butterworth-Heinemann, pp. 24 – 62, 1994.

Smith, R. W., "AUSM(ALE): A Geometrically conservative Arbitrary Lagrangian-Eulerian Flux Splitting Scheme," *Journal of Computational Physics*, 150, 268 – 286, 1999.

Sod, G. A., "A survey of Several Finite Difference Methods for Systems of Nonlinear Hyperbolic Conservation Laws," *Journal of Computational Physics*, 27, 1 – 31, 1978.

Sweby P. K., "High Resolution Schemes using Flux Limiters for Hyperbolic Conservation Laws," *SIAM Journal on Numerical Analysis*, 21, 995 – 1011, 1984.

Tai, C. H., Chiang, D. C., Su, Y. P., "Explicit Time Marching Methods for The Time-Dependent Euler

Computations," *Journal of Computational Physics*, 130, 191 – 202, 1997.

Tannehill, J. C., Muge P. H., "Improved Curve Fits for the Thermodynamic Properties Equilibrium Air Suitable for Numerical Computation using Time Dependent and Shock-Capturing Methods," *NASA CR-2470*, 1974.

van der Vegt, J. J. W., van der Ven, H. "Space-Time Discontinuous Galerkin Finite Element Method with Dynamic Grid Motion for Inviscid Compressible Flows: I. General Formulation," *Journal of Computational Physics*, 182, 546 – 585, 2002a.

van der Vegt, J. J. W., van der Ven, H. "Space-Time Discontinuous Galerkin Finite Element Method with Dynamic Grid Motion for Inviscid Compressible Flows: II. Efficient Flux Quadrature," *Computer Methods in Applied Mechanics and Engineering*, 191, 4747 – 4780, 2002b.

van Leer, B., "Flux-Vector Splitting for the Euler Equations," *Lecture Notes in Physics*, Springer - Verlag, 170, 507 – 512, 1982.



Emre Alpman was born on April 10th, 1977 in Ankara. He completed his high school education in 1995 at the Ankara Gazi Anatolian High School. He attended Aeronautical Engineering Department of Middle East Technical University the in the same year and graduated with the first rank in 1999. After graduation he enrolled to the Master of Science program of Middle East Technical University Aerospace Engineering Department and completed this program in 2001. In 2002 he entered the Pennsylvania State University Aerospace Engineering Department to seek a doctorate degree, which he received in 2006 by graduating from the program. On December 2006 he joined Marmara University Mechanical Engineering Department as an Assistant Professor. Currently, he continues to work in this position.